Trajectory Planning for Connected and Automated Vehicles: Cruising, Lane Changing, and Platooning

Xiangguo Liu,[1] Guangchen Zhao,[2] Neda Masoud,[3] and Qi Zhu[1]

[1]Northwestern University, USA
[2]University of Maryland, USA
[3]University of Michigan, USA

Abstract

Autonomy and connectivity are considered among the most promising technologies to improve safety and mobility and reduce fuel consumption and travel delay in transportation systems. In this paper, we devise an optimal control-based trajectory planning model that can provide safe and efficient trajectories for the subject vehicle while incorporating platoon formation and lane-changing decisions. We embed this trajectory planning model in a simulation framework to quantify its fuel efficiency and travel time reduction benefits for the subject vehicle in a dynamic traffic environment. Specifically, we compare and analyze the statistical performance of different controller designs in which lane changing or platooning may be enabled, under different values of time (VoTs) for travelers. Results from extensive numerical experiments indicate that our design can not only provide first-hand cost savings for the subject vehicle but also second-hand savings for vehicles upstream of the subject vehicle. Experiments also highlight that lane changing and platooning can both offer benefits, depending on the relative values of fuel cost and the traveler's VoT: with a small VoT, the fuel efficiency benefits of platooning outweigh time savings offered by lane changing. However, a vehicle with a high VoT may find it more beneficial to travel outside of a platoon and complete its trip faster by leveraging lane changes.

Introduction

It is envisioned that, in the near future, transportation systems would be composed of vehicles with varying levels of connectivity and autonomy. Connected vehicle (CV) technology facilitates communication among vehicles, the infrastructure, and other road users [1], allowing vehicles to *see* beyond the driver's line of sight and the transportation infrastructure to be proactive in responding to stochastic changes in road conditions and travel demand [2].

Automated vehicle technology enables automation of vehicles at different levels, where Level 0 automation indicates no automation; Automation levels 1 and 2 refer to a single and multiple driving-assistance systems being present in the vehicle, respectively. Level 3 automation allows the transfer of control authority between the human driver and the autonomous entity when the automation fails. Level 4 autonomy allows for the vehicle to control all functionalities within specified regions. Finally, in level 5 autonomy vehicles can travel anywhere without any intervention from human drivers [3].

Although the connected and automated vehicle (CAV) technologies can each be deployed independently in a vehicle, when combined they can provide a synergistic effect that goes beyond the sum of their individual benefits. It is expected that upon deployment, the CAV technology could significantly improve mobility, enhance safety and traffic flow stability, reduce congestion, and improve fuel economy, among other benefits [4, 5, 6, 7, 8]. The degree to which such benefits can be realized in real-world conditions depends on a wide array of factors, among which trajectory planning of CAVs plays a major role [9]. The main purpose of trajectory planning is to provide a vehicle with a collision-free path, considering the vehicle dynamics, the surrounding traffic environment, and traffic rules [10]. More comprehensive works could incorporate secondary objectives such as achieving fuel economy [11, 12, 13, 14, 15] and time efficiency [16, 17].

Platooning is one of the applications of the CAV technology, which allows for vehicles to travel with small gaps between them, thereby reducing the aerodynamic drag on platoon members and increasing fuel efficiency [18]. To enjoy the benefits of platooning, the trajectory planning methods should be enhanced to include platooning decisions, including (1) whether a vehicle should merge into a platoon, and (2) among the existing platoons, which platoon should a vehicle join, among others. Additionally, in the existence of platoons, lane changing becomes a more complex task: for a platoon member to join lanes, they should dissolve from the platoon and incur the energy cost of such a decision. Furthermore, a decision on the part of a vehicle to dissolve from a platoon will impact the energy efficiency of other platoon members. Similarly, merging into a platoon may require changing lanes, which could offset some of the fuel efficiency benefits of platooning. Therefore, accounting for platoon-merging and lane-changing decisions is a critical part of trajectory planning in the era of CAV technology.

There are a number of classical methods on trajectory planning, such as sampling based [19, 20], optimization based [21, 22], and graph search based [23]. These studies and their potential for use in CAV systems will be discussed in detail in the Related Works section. Despite the high performance of these methods on trajectory planning, the transportation systems of the future are expected to have high levels of autonomy and connectivity, thereby requiring the existing methods to be reviewed and reevaluated within this new context. More precisely, although current methods can plan vehicles' lateral and longitudinal positions, they need to be enhanced to explicitly make discrete decisions on platoon merging and lane changing jointly with continuous decisions on trajectory planning. The contributions of this paper are as follows:

- We put forward a joint cruising, lane changing, and platoon-merging planner for a CAV, in a dynamic environment with a mixed traffic consisting of connected and legacy vehicles. The planner is capable of planning the future geo-coordinates of the vehicle jointly with lane-changing and platoon-merging decisions.

- We develop a simulation environment for traffic dynamics, in which vehicles may enter or exit the traffic stream, merge into or split from a platoon, change lanes, and adjust their velocities.

- We demonstrate that the subject vehicle (which is assumed to be connected and automated) can obtain statistically significant fuel and time savings through extensive simulations in various traffic states (i.e., free-flow, onset-of-congestion, and congested).

- We demonstrate that legacy vehicles traveling upstream the subject vehicle can obtain statistically significant fuel efficiency benefits.

- We evaluate the performance of our design under different minimum platoon-keeping distance requirements and values of time (VoTs) for travelers.

The rest of the article is organized as follows: First, we review the literature on trajectory planning. Then, we formulate an optimal control model for planning the trajectory of a CAV. Next, we present a general framework for the study and our assumptions, as well as a simulation environment that consists of a two-lane highway with multiple on- and off-ramps and a dynamic traffic stream. In particular, we describe how vehicles with various levels of autonomy and connectivity interact with each other in the simulation environment. Finally, we conduct a series of analyses under various traffic conditions to quantify the fuel-efficiency benefits of our approach for the subject vehicle, as well as those of its surrounding vehicles within platoons and as free agents. We end the paper by summarizing the takeaways.

Related Works

Traditionally, trajectory planning has been mainly based on vehicle dynamics constraints, such as acceleration range and steering performance. More advanced driving assistance

TABLE 1 Summary of parameters.

Parameter	Value	Definition
t_{upd}	0.4 s	Updating period of the trajectory of the subject vehicle
p_{on}	0.6	The possibility that a vehicle is interested in joining the freeway from an on-ramp
p_{off}	0.6	The possibility that a vehicle is interested in taking an off-ramp
p_{npe}	0.5	The possibility that the vehicle is a non-platoon-enabled vehicle
p_{merge}	0.6	The possibility that a vehicle intends to merge
p_{change}	0.1	The probability that the vehicle intends to change lane
t_p	3.5 s	Time gap between two successive vehicles that are not in a platoon
t_g	0.55 s	Time gap between two successive vehicles in a platoon
t_{lcp}	3.6 s	Surrounding vehicles finish lane changing within this time
t_{lc}	5 s	The minimum time interval between two successive lane changes by successive vehicles
τ_s	0.4 s	Updating period of the trajectory of surrounding vehicles
τ_{cf}	1.0 s	Reaction time delay in the car-following model
$t_{N_{act}}$	10 s	Prediction horizon in the optimal control model
v_m^{le}	20 m/s	The velocity in left the lane when it reaches the maximum flow
v_m^{ri}	14 m/s	The velocity in the right lane when it reaches the maximum flow
v_{max}^{le}	30 m/s	The maximum velocity in the left lane
v_{max}^{ri}	20 m/s	The maximum velocity in the right lane
a_{max}	2 m/s^2	The maximum acceleration for the subject vehicle
j_{max}	3.5 m/s^3	The maximum jerk for the subject vehicle
d_{cg}	50 m	The critical gap decides whether it is feasible to change lane
l_{car}	5 m	Length of a vehicle
h_{st}	5 m	The vehicle would stop at headway of this value
a	2 m/s^2	The maximum desired acceleration
b	3 m/s^2	The comfortable deceleration
γ_{AR}	0.3987	Coefficient for air resistance force
γ_{RR}	281.547	Coefficient for rolling resistance force
γ_{GR}	0	Coefficient for grade resistance force
γ_{IR}	1750	Coefficient for inertia resistance force
η_f	5.98×10^{-8} dollars/J	Fuel cost for a unit energy consumed by the vehicle
P_{sch}	{2,10,50}	The scheduled splitting position can be 2, 10, or 50 road pieces later
$\mathcal{N}(\mu_{sch},\sigma_{sch})$	$\mathcal{N}$ (2, 5), left, $\mathcal{N}$ (−1, 5), right	The norm distribution of the scheduled splitting position in two lanes, respectively

systems, e.g., adaptive cruise control (ACC), enhance trajectory planning through utilizing data collected by the vehicle's onboard sensors. CV technology provides an opportunity to incorporate more diverse types of data (e.g., weather conditions) from a wider spatial range (e.g., from objects beyond the line of sight of the vehicle). However, there is a need to develop algorithmic tools that can incorporate this information into trajectory planning. Several attempts, such as Connected Cruise Control [32, 33] and Cooperative Adaptive Cruise Control (CACC) [34, 35, 36, 37] have been made to incorporate vehicle-to-vehicle (V2V) communications into trajectory planning. CACC is one of the most promising technologies that allows CVs to autonomously, and without the need for a central management system, plan their trajectories using V2V communications [38]. The information flow topology in a CACC system typically includes predecessor following, predecessor-leader following, bidirectional

topology, etc. [39]. Advanced communication protocols, such as Dedicated Short-Range Communications (DSRC), LTE, and 5G are proposed and developed to improve the communication bandwidth of V2V communications [40, 41, 42].

Table 2 summarizes recent studies in the literature that have focused on trajectory planning of CAVs, with different levels of automation. This table points out multiple attributes of these studies, including whether obstacles are dynamic or not, the environment geometry, whether the ego vehicle is capable of platoon formation, whether lateral motion is considered or not, the penetration rate of CVs, and their cost functions. The rest of this section elaborates on the specifics of these attributes.

The ultimate goal of trajectory planning is to enable vehicles to travel safely and efficiently in real traffic conditions. Therefore, different trajectory planning algorithms are developed for implementation in different contexts to capture

TABLE 2 Overview of the trajectory planning literature.

Study	Obstacle	Environment	Platoon	Lateral motion	Connectivity	Cost			
						Tracking	Fuel	Time	Comfort/ safety
[24]	Dynamic	Curvy lanes	No	Yes	No	Yes	No	No	Yes
[11]	Static	Routes	No	No	No	No	Yes	No	No
[25]	Dynamic	Curvy lanes	No	Yes	No	No	No	No	Yes
[26]	Dynamic	Lanes	Yes	Yes	Partial	Yes	No	No	No
[27]	Dynamic	Curvy lanes	No	No	No	No	No	No	Yes
[28]	Dynamic	Lanes	Yes	Yes	Full	No	Yes	Yes	Yes
[29]	Static	Curvy lanes	No	No	No	Yes	No	No	No
[23]	Dynamic	Curvy lanes	No	Yes	No	Yes	No	No	Yes
[19]	Dynamic	Curvy lanes	No	Yes	No	No	No	Yes	Yes
[20]	Static	Free space	No	Yes	No	No	No	No	Yes
[30]	Dynamic	Curvy lanes	No	Yes	No	No	No	No	Yes
[31]	Static	Curvy lanes	No	Yes	No	No	No	Yes	Yes
This article	**Dynamic**	Lanes	**Yes**	**Yes**	**Partial**	No	**Yes**	**Yes**	**Yes**

© SAE International

different abstractions of real-world conditions, e.g., obstacles, curved roads, signal lights, and mixed traffic components [43]. In [24], Gu et al. focus on the subject vehicle's movement around a single static obstacle, and its distance-keeping and overtaking of a single leading vehicle. [11] proposes a dynamic programming algorithm for speed planning in a transportation network with stop signs and traffic lights. [27] presents a method that exploits the complete permissible road width in curvy road segments to increase driving comfort and safety through minimized steering actuation. [26, 28] consider the impact of surrounding vehicles with fixed velocity on the trajectory planning of the subject vehicle. In general, the degree to which different models are set to imitate real traffic conditions depends on research priorities. The closer the environment can resemble real-world conditions the higher the accuracy and reliability of trajectory planning, but the higher the computational complexity and the worse the real-time performance. [44] reviews planning and control algorithms for self-driving vehicles in urban environment and highway scenarios. A review of the existing studies reveals that, in general, the literature is very limited in capturing the dynamics of the driving environment. In our work, we develop a trajectory planning method for a general highway system based on the work by [22]. However, we add several components, such as on-ramps and off-ramps, lane-changing capability, speed adjusting, and penetration of platoons, to more accurately simulate the surrounding traffic environment.

Lane changing is another important component of trajectory planning. Lane changing is one of the most challenging driving maneuvers for researchers to understand and predict, and one of the main causes of congestion and collisions in the transportation system [45]. The real-time information received from the driving environment and other road users

can be used to facilitate lane-changing maneuvers that enhance safety, comfort, and traffic efficiency [22]. [46] propose a distributed algorithm to make lane-changing decisions. The authors claim that this mechanism can maximize the number of safe lane changes within the entire system. However, they did not demonstrate the level of improvement in system-level performance. The developments in lane-changing models before 2014 are comprehensively reviewed in [47, 48]. Zheng et al. [48] claim that in real lane-changing situations, drivers can simultaneously monitor and evaluate multiple spacings in the target lane and make a decision on where and how to execute the lane change. In [45], two types of games are proposed for modeling the lane-changing behavior: under complete information in the presence of CV technology and under incomplete information in its absence. Simulation results indicate that the game theoretic-based lane-changing models are more realistic than the basic gap-acceptance model and the MOBIL model. Wang et al. [49] proposed a predictive model for lane-changing control that considers both discrete lane-changing decisions and continuous acceleration values. The lane-changing method proposed by Luo et al. in 2016 [22] executes lane-changing maneuvers; however, their model is not capable of making lane-changing decisions. A review of the existing work on lane changing demonstrates that most research in this area focuses either on when or where to change lanes or on the execution of lane changing after the decision to change lanes has been made. Nilsson et al. [50] propose a lane-changing method composed of three steps, that is, deciding whether to change lanes, selecting the target position and the time instance to initiate the lane changing process, and planning the trajectory. However, these three steps are followed sequentially. In contrast, in our work, we make all three decisions

concurrently in an integrated framework to minimize fuel and time costs. We move the state of the art one step forward by evaluating multiple spacings in the target lane from the viewpoint of the feasibility of maneuvering, safety, and efficiency. Furthermore, we evaluate the effects of lane changing in long-distance travels in a dynamic system.

Platooning makes one of the most interesting and important components of trajectory planning in the next generation of transportation systems. The capability to incorporate platooning is another factor that differentiates existing trajectory planning methods. Platooning is a specific application of the CV technology that can introduce a wide range of vehicle- and system-level benefits. A platoon is a single-file line (i.e., a virtual train) of vehicles that, owing to constant communication, are able to travel with small gaps between them. Platoon formation can introduce many benefits including (i) Energy efficiency through reducing the aerodynamic drag force on platoon members [51, 52]; (ii) Reducing emissions [53]; (iii) Increasing road capacity through reducing the headways between vehicles; (iv) Reducing stochasticity in the traffic stream by having platoon members follow the platoon leader, thereby reducing the likelihood of highway traffic breakdown, improving travel times, and increasing travel time reliability [54, 55]; (v) Facilitating real-time management of traffic and improving mobility by aggregating the unit of traffic from an individual vehicle to a cluster of vehicles. Table 2 lists studies in the literature that incorporate platooning. Note that "yes" for the field "platoon" in this table indicates the capability of platoon formation, rather than platoon control strategies [56, 57] or intra-platoon communication [58, 59]. In our work, we model possible platoon formations between the subject vehicle and its surrounding vehicles. Furthermore, our method will make merging/splitting decisions along with trajectory planning.

The ability to capture the heterogeneity in the level of connectivity and autonomy of vehicles is another factor that differentiates existing trajectory planning methods, as described in Table 2. Finally, trajectory planning methods are different in terms of their objective function. In general, the goal is to find the least-cost trajectory, where the cost function could include any combination of the following components: time cost of the trip (i.e., trip length), fuel consumption, comfort and safety of onboard passengers, and precision in tracking (i.e., the degree to which the vehicle deviates from a prespecified ideal trajectory).

There are a number of comprehensive reviews on path planning, maneuver choice, and trajectory planning [60, 61]. A more recent work utilizes optimal control to plan trajectories for automated vehicles, where they leverage dynamic programming to provide an initial trajectory based on a simplified optimal control problem [62]. However, they do not consider platooning, which is envisioned to be an important component of future traffic streams, nor do they consider the benefits of utilizing optimal trajectories, neither through simulations nor through real-world experiments.

Methods

The goal of this study is to design an optimal control-based trajectory planning model that can be utilized by an automated (level 2 or higher autonomy) vehicle, hereafter referred to as the *subject vehicle.* The optimal control model will be designed to incorporate microscopic traffic information from the traffic stream in the local neighborhood of the subject vehicle, with the goal of devising fuel- and time-efficient trajectories that may include merging into a platoon and changing lanes. We start this section by describing the optimal control model. We then describe the general framework and our assumptions, as well as a simulation environment that we will use to quantify the overall cost savings for the subject vehicle and its surrounding traffic.

Optimal Control Model

In this section, we devise an optimal control model to determine the trajectory of the subject vehicle in real time. It is noted that this work focuses more on decision-making and trajectory planning, rather than trajectory tracking, so we simplify the vehicle dynamics model as a mass point and assume we can directly control its longitudinal and lateral acceleration, and thereby its trajectory. The proposed optimal control model is probably safe and is designed to account for fuel and time efficiency, as well as comfort of onboard passengers.

The optimal control model is a nonlinear optimization model. The state variables of this model include longitudinal and lateral positions, platoon membership status (whether or not in a platoon, and the scheduled splitting time if a platoon member), and the control variables are longitudinal and lateral accelerations, the binary decision to join a platoon and the binary decision to change lanes. While adjusting acceleration can be considered as a single action that can be almost instantaneously carried out, a change in lane position and platoon membership is a lengthier process and may require multiple sub-actions, as described in Table 3. As demonstrated in this table, at each time step the subject vehicle can be in one of the following six states: (*i*) "left lane; free agent," indicating that the vehicle is in the left lane and is not part of any platoon; (*ii*) "right lane; free agent," indicating that the vehicle is in the right lane and is not part of any platoon; (*iii*) "left lane; in platoon (active)," indicating that the subject vehicle is in the left lane and is the platoon leader, and the scheduled platoon splitting position has not yet reached; (*iv*) "right lane; in platoon (active)," indicating that the subject vehicle is in the right lane and is the platoon leader, and the scheduled platoon splitting position has not yet reached; (*v*) "left lane; in platoon (passive)," indicating that the subject vehicle is in the left lane, the platoon splitting position has reached, and the platoon the subject vehicle

TABLE 3 Sub-action sequences for each state-action tuple.

Initial state	Target state	Sub-action sequence
Left lane; free agent	Left lane; free agent	Wait
	Left lane; in platoon	Merge→wait
	Right lane; free agent	Wait→lane change→wait
	Right lane; in platoon	Wait→lane change→merge→wait
Right lane; free agent	Left lane; free agent	Wait→lane change→wait
	Left lane; in platoon	Wait→lane change→merge→wait
	Right lane; free agent	Wait
	Right lane; in platoon	Merge→wait
Left lane; in platoon (active)	Left lane; free agent	Split→wait
	Left lane; in platoon	Wait
	Right lane; free agent	Split→wait→lane change→wait
	Right lane; in platoon	Split→wait→lane change→merge→wait
Right lane; in platoon (active)	Left lane; free agent	Split→wait→lane change→wait
	Left lane; in platoon	Split→wait→lane change→merge→wait
	Right lane; free agent	Split→wait
	Right lane; in platoon	Wait
Left lane; in platoon (passive)	Left lane; free agent	Split→wait
	Left lane; in platoon	Split→wait→merge→wait
	Right lane; free agent	Split→wait→lane change→wait
	Right lane; in platoon	Split→wait→lane change→merge→wait
Right lane; in platoon (passive)	Left lane; free agent	Split→wait→lane change→wait
	Left lane; in platoon	Split→wait→lane change→merge→wait
	Right lane; free agent	Split→wait
	Right lane; in platoon`	Split→wait→merge→wait

© SAE International

was formerly leading is in the process of dissolving; (*vi*) "right lane; in platoon (passive)," indicating that the subject vehicle is in the right lane, the platoon splitting position has reached, and the platoon the subject vehicle was formerly leading is in the process of dissolving.

Table 3 shows that at each time step, the subject vehicle switches from its current state to a target state. Depending on its initial and target states, the subject vehicle may need to complete a sequence of sub-actions, including "wait," "merge," "split," and "lane change." The "wait" sub-action indicates that the vehicle needs to maintain its state after completing its previous sub-action. The sub-actions "merge" and "split" indicate merging into a platoon and splitting from a platoon, respectively. Finally, the "lane change" sub-action indicates changing lanes. For example, if the target state "right lane; in platoon" is the selected action under the current state "left lane; in platoon (active)," then the subject vehicle needs to complete the sequence of sub-actions "split→wait→lane change→merge→wait."

The Trajectory Function
Following [22], we use a quintic function, based on time, as our trajectory function for each sub-action. The quintic function is selected because it guarantees a smooth overall trajectory, even with multiple different sub-actions. Equation 1 shows the trajectory function,

$$
\begin{cases}
x(t) = \sum_{i=1}^{N_{act}} (a_5^i t^5 + a_4^i t^4 \\
\qquad + a_3^i t^3 + a_2^i t^2 + a_1^i t + a_0^i) f_i(t) \\
y(t) = \sum_{i=1}^{N_{act}} (b_5^i t^5 + b_4^i t^4 \\
\qquad + b_3^i t^3 + b_2^i t^2 + b_1^i t + b_0^i) f_i(t)
\end{cases}, \qquad \text{Eq. (1)}
$$

where $x(t)$ and $y(t)$ indicate the longitudinal and lateral positions of the vehicle at time t, respectively, and N_{act} denotes the number of sub-actions the subject vehicle needs to complete. Coefficients a_0^i through a_5^i and b_0^i through a_5^i are decision variables that determine the optimal solution. Function $f_i(t)$ may be formulated as

$$
f_i(t) = \begin{cases} 1 & t_{i-1} \le t < t_i \\ 0 & \text{otherwise} \end{cases} \qquad \text{Eq. (2)}
$$

where $[t_{i-1}, t_i]$ is the time window for completing the ith sub-action, and $t_{N_{act}}$ is the prediction horizon.

Boundary Conditions For every sub-action, the following boundary conditions must be satisfied,

$$\begin{cases} x(t_{i-1}) = x_{t_{i-1}}, \dot{x}(t_{i-1}) = v_{x,t_{i-1}}, \ddot{x}(t_{i-1}) = a_{x,t_{i-1}}, \\ y(t_{i-1}) = y_{t_{i-1}}, \dot{y}(t_{i-1}) = v_{y,t_{i-1}}, \ddot{y}(t_{i-1}) = a_{y,t_{i-1}} \end{cases} \quad \text{Eq. (3)}$$

$$\begin{cases} x(t_i) = x_{t_i}, \dot{x}(t_i) = v_{x,t_i}, \ddot{x}(t_i) = a_{x,t_i} \\ y(t_i) = y_{t_i}, \dot{y}(t_i) = v_{y,t_i}, \ddot{y}(t_i) = a_{y,t_i} \end{cases} \quad \text{Eq. (4)}$$

where t_{i-1} and t_i are the starting and ending time for the ith sub-action, respectively, and $x_{t_{i-1}}$, $v_{x,t_{i-1}}$, $a_{x,t_{i-1}}$, $y_{t_{i-1}}$, $v_{y,t_{i-1}}$, and $a_{y,t_{i-1}}$ are the longitudinal and lateral geo-coordinates, velocity, and acceleration for the starting point of the sub-action, respectively. These values are accordant with the ending point for the last sub-action. For each sub-action, the longitudinal coordinate, velocity, and acceleration at the end of the sub-action, as well as the duration of the sub-action are all free variables that are optimized.

Constraint Sets There are a number of constraints on the position, speed, acceleration, and jerk of the subject vehicle elaborated in the following.

1. *Speed limitation:* The longitudinal speed of the subject vehicle should be no more than the maximum speed in its lane, and should always be non-negative, as presented in Equation 5:

$$0 \leq v_x(t) = \dot{x}(t) \leq v_{x,\max}^l, \quad \text{Eq. (5)}$$

where $v_x(t)$ denotes the longitudinal speed of the subject vehicle, l indicates the lane in which the vehicle is traveling, and $v_{x,\max}^l$ denotes the maximum vehicle speed in lane l.

2. *Collision avoidance:* The subject vehicle should maintain a minimum time gap (denoted by t_{safe}) from its immediate downstream vehicle during all sub-actions in all t, as indicated in Equation 6,

$$x_L(t) - x_{\text{sub}}(t) > t_{\text{safe}} \ v_{\text{sub}}(t) + l_{\text{car}}, \forall t \in \left[t_0, t_{N_{\text{act}}} \right], \text{Eq. (6)}$$

where $x_L(t)$ is the position of the immediate downstream vehicle (i.e., the leader); $x_{\text{sub}}(t)$ and $v_{\text{sub}}(t)$ are the position and velocity of the subject vehicle, respectively; and l_{car} is the vehicle length.

3. *Acceleration bound:* During all sub-actions, the longitudinal or lateral acceleration of the subject vehicle cannot exceed a maximum value due to mechanical performance limitations and safety considerations. This constraint is enforced in Equation 7,

$$\left| a_{x,y} \right| = \left| \dot{v}_{x,y} \right| < a_{\max}, \quad \text{Eq. (7)}$$

where $v_{x,y}$ is the velocity vector and $a_{\max}$ is the maximum acceleration.

4. *Jerk bound:* Since the subject vehicle's jerk directly influences the comfort level and safety of its onboard passengers, we bound the jerk by a maximum value as stated in Equation 8,

$$\left| j_{x,y} \right| = \left| \ddot{v}_{x,y} \right| < j_{\max}, \quad \text{Eq. (8)}$$

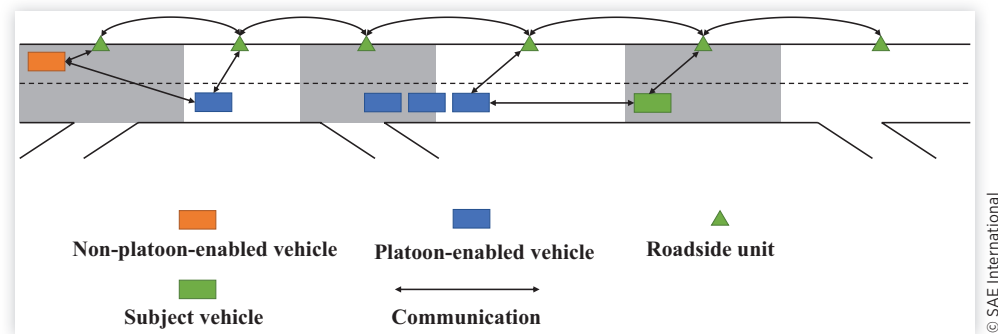where $j_{\max}$ is the maximum jerk.

Objective Function We define the objective function as a linear combination of fuel and time costs, as stated in Equation 9,

$$C_{\text{overall}} = \min \left\{ \eta_f \sum_{i=1}^{N_{\text{act}}} \beta(i) \int_{t_{i-1}}^{t_i} \left(\gamma_{\text{AR}} v^2(t) + \gamma_{\text{RR}} \right. \right.$$
$$\left. \left. + \gamma_{\text{GR}} + \gamma_{\text{IR}} \left(a(t) \right)_+ \right) v(t) dt + \eta_t \sum_{i=1}^{N_{\text{act}}} \left(t_i - t_{i-1} \right) \right\} \quad \text{Eq. (9)}$$

The four terms $\gamma_{\text{AR}} v^2(t)$, γ_{RR}, γ_{GR}, and $\gamma_{\text{IR}}(a(t))_+$ are the aerodynamic resistance force, rolling resistance force, grade resistance force, and inertia resistance force, respectively. For detailed expressions of these forces, we refer the reader to [63]. The parameter η_f is the fuel cost for a unit energy consumed by the vehicle and is measured in dollars. The parameter η_t is the unit cost of time, also known as value of time, VoT), and is measured in dollars per unit of time, e.g., a second. The parameter $\beta(i)$ indicates the fuel-saving coefficient for sub-action i. As reported in [51], fuel-saving percentage varies from 3% to 30% at different spacings with a different number of vehicles in a platoon in highway scenarios. Additionally, vehicles in the middle of a platoon (i.e., not at the head or tail of a platoon) experience the most fuel savings. The platoon tail is the second-best position in terms of fuel saving, and the platoon leader has the least fuel saving. Here, for simplicity, we assume a 10% fuel saving for all vehicles in a platoon, and a 5% fuel saving when a vehicle engages in merging or splitting processes. Thus, we set $\beta(i) = 1$ for a free agent, and $\beta(i) = 0.9$ for a platoon member. Furthermore, we set $\beta(i) = 0.95$ for split and merge sub-actions because, in the transition state to and from a platoon, vehicles still experience fuel savings, but not to the same extent as a platoon member. Note that despite the platoon-related fuel efficiency benefits of the merge and split processes, the change in velocity during the merge and split processes may lead to higher fuel consumption levels. However, the optimization problem would naturally account for such trade-offs.

General Framework and Assumptions

In this study, we consider a mixed traffic stream with various levels of autonomy. Specifically, we model both vehicles that

FIGURE 1 The communication and control framework.

Non-platoon-enabled vehicle   Platoon-enabled vehicle   Roadside unit

Subject vehicle   Communication

© SAE International

are human-driven and not platoon-enabled, and platoon-enabled vehicles. A platoon-enabled vehicle is a vehicle that has level 2 or higher autonomy (and is equipped with distance sensing and keeping technology such as ACC) according to the Society of Automotive Engineer's (SAE's) classification. Furthermore, in this study we assume that all vehicles are connected, that is, all vehicles can communicate with each other and with roadside units (RSUs) using DSRC devices, with a reliable communication range of 300 m. Figure 1 demonstrates the communication and control framework of our work.

To develop a simulation environment for the system, we divide the transportation network into a number of *road pieces.* We define a road piece as a section of a road that satisfies the following two conditions: (*i*) The macroscopic traffic conditions, to which we refer as "traffic states," are likely to be homogeneous within a road piece. For example, on a highway segment the traffic conditions around on-ramps and off-ramps are typically different from their upstream and downstream segments, indicating that on-ramps and off-ramps require dedicated road pieces; (*ii*) Vehicles within a road piece are able to communicate with each other, either directly or through RSUs. This requirement implies that, in the case of DSRC-enabled communication, the length of a road piece cannot exceed 600 m so as to enable all vehicles to stay connected using a single RSU located in the middle of the road piece. Limiting the length of a road piece ensures that, with strategic positioning of RSUs, all CVs can receive microscopic traffic information of their neighbors (i.e., geo-coordinates, velocity, acceleration, braking, steering angle, etc.) and use this information to plan more informed and efficient trajectories.

In our modeling of a traffic stream characterized with full connectivity and a heterogeneous level of autonomy, we account for the delay between the occurrence of a stimulus and the execution of an action in response to it. In the case of a human driver, this delay is referred to as the perception-reaction time [64] and accounts for the perception delay (either by the driver or from the part of the vehicle sensors), the decision-making delay, and the execution delay. In the case of the autonomous entity being in charge, this delay can be attributed to sensory delay, delay in the communication network, computational time, and actuation delay.

Surrounding Vehicles Surrounding vehicles' trajectories will be simulated based on a microscopic car-following model so as to reflect a realistic and dynamic traffic environment. The surrounding traffic information will get updated every $\tau_s = 0.4$ s. Note that the value of τ is selected based on the human perception-reaction time, which is within the range of 0.3-1.5 s [65]. However, this is a parameter that can be easily adjusted in the model. At each updating step, four functions will be executed by the surrounding vehicles in the following sequence: join/exit from the highway, merge into/split from a platoon, change lanes, and adjust velocity based on a car-following model. These functions are elaborated in the following.

1. *Join/exit from the highway:* We assume that the probability that a vehicle enters the highway from an on-ramp at each updating step is p_{on}. The vehicle is assumed to be able to join the highway if it can maintain a minimum time gap of length t_p from the vehicles both upstream and downstream of the ramp entry point in the right lane of the highway. We set the speed of this entering vehicle similar to the speed of its downstream vehicle. Moreover, we set the probability of the vehicle not being a platoon-enabled vehicle as p_{npe}.

   At each update step, a vehicle can leave the highway if the following three conditions are satisfied: (1) it is traveling on the right lane of the highway, (2) it is located at the upstream of an off-ramp point, and (3) the time gap between the vehicle and the off-ramp point is smaller than the update step τ_s. Among all vehicles that satisfy these conditions, we assume the probability that one vehicle intends to leave the highway is p_{off}. This exiting vehicle and its profile is directly taken off the current iteration.

2. *Merge into/split from a platoon:* To ensure that our model remains computationally tractable, we assume that a vehicle could hold only a single platoon membership status (either a member or not a member) throughout a road piece, i.e., the merging or splitting process can only commence in the transition point between two road pieces. A vehicle can merge into a platoon when it is already a platoon leader (resulting in the merging of two platoons), or a

platoon-enabled free agent. Among all vehicles that qualify to merge into a platoon, the probability that a vehicle intends to merge is assumed to be p_{merge}. There are two cases regarding the profile of the vehicle in the immediate downstream of the merging vehicle. If it is a platoon member, then the new merging vehicle will have the same scheduled splitting position as other vehicles in the platoon. If it is a free agent, the scheduled splitting position P_{sch}, in the units of number of road pieces, will be decided at this time using a normal distribution. (For more details, see section "Platoon membership.")

Every time when a platoon passes the transition point of two road pieces, the scheduled splitting position will decrease by 1 unit until this value reaches 0, at which point the platoon would split into free agents.

3. *Lane change:* Rahman et al. [47] provide a comprehensive review of prior work on lane-changing models. For simplicity, in this paper we adopt the random lane-changing model, in which vehicles may change lanes once a minimum gap criterion is satisfied. We assume that, in every update step, at most a single vehicle can change lanes. Furthermore, for safety considerations, we require a minimum time (no less than $t_{\text{lc}} = 5$ s) between two successive lane changes by two successive vehicles (immediate follower/leader) traveling in the same lane. We allow only free agents, and not platoons, to change lanes. The gap between the lane-changing vehicle and surrounding vehicles (the leading vehicle in the same lane, and the leading and following vehicles in the target lane) should be at least d_{cg} to ensure a safe lane-changing maneuver. Finally, the following vehicle in the target lane cannot be a follower in a platoon, indicating that the lane-changing process cannot insert vehicles into a platoon.

Not all vehicles that satisfy the conditions above intend to change lanes. Among all qualified vehicles, the probability that a vehicle intends to change lane is p_{change}. The lane-changing process is assumed to be completed within t_{lcp} seconds, after which the lateral position of the lane-changing vehicle would not change, and its longitudinal speed has to have reached the speed of the leading vehicle in the target lane.

4. *Adjusting velocity using a car-following model:* Each vehicle needs to continuously adjust its velocity to maintain a large-enough safety gap from its leading vehicle. For a free agent we use the Intelligent Driver Model (IDM) [66] for adjusting velocity. For platoon members in the steady state, the platoon leader will behave similarly to a free agent in terms of car-following behavior, and other platoon members will instantaneously take the same acceleration and velocity as the platoon leader to maintain a steady headway to their preceding vehicle. In the splitting/merging state, the headway will increase/decrease following a constant speed. (We use the speed of 5 m/s in our simulations.) The parameters used to calibrate IDM are summarized in Table 1. For more

information on the car-following model parameters, we refer the reader to [66]. For more information on the optimal control model parameters, we refer the reader to [22]. For fuel cost-related parameters, we refer the reader to [51, 63].

Subject Vehicle The subject vehicle updates its motion plan every $t_{\text{upd}} = 0.4$ s. It is assumed that the surrounding vehicles' motion information is available to the subject vehicle in real time. Due to the long computational time of trajectory planning and control in a dynamic driving environment, it is problematic for the subject vehicle to obtain the latest traffic information and then plan its own trajectory for the immediate next period, that is, after the trajectory planning process is completed, the planned trajectory would be already outdated. Thus we implement a receding horizon control method and consider the computational delay explicitly in this paper. During this process, the subject vehicle perceives the environment, estimates other vehicles' motions for the next $2t_{\text{upd}}$ period, and makes its own trajectory plan for the second following period, i.e., $[t + t_{\text{upd}}, t + 2t_{\text{upd}}]$, where t is the current time. This results in a trajectory that can still be effectively followed during this window. The potential mismatch between the estimated and actual trajectories of the surrounding vehicles can be addressed by adopting the receding horizon planning approach. The optimal trajectory is computed by a non-convex optimization solver in MATLAB, called fmincon.

As discussed in [22], the subject vehicle may get involved in a collision due to the surrounding vehicles' sudden speed fluctuations during the lane-changing process. More specifically, the subject vehicle may not be able to take any action without violating the constraints of the optimal control model for the following reasons: (*i*) sudden speed change of the surrounding vehicles; (*ii*) comfort-related maximum acceleration and jerk constraints in the optimal control model; and (*iii*) conservative constraints regarding the safety time gap between the subject vehicle and any surrounding vehicles. In case of there being no feasible solution for the optimal control model, the Intelligent Driver car-following Model is utilized to provide a longitudinal motion reference for the subject vehicle.

Platoon Membership This section elaborates on platoon formations. When merging, we assume a free agent or a platoon can merge with its immediate downstream free agent or platoon, that is, merging can occur between two free agents, two platoons, or a free agent and a platoon. For the purpose of simulations, we assume a finite number of possible scheduled splitting positions, $\ell_{\text{sch}}^1, \ell_{\text{sch}}^2, \cdots, \ell_{\text{sch}}^n$, in an ascending order of time. Given the mean μ_{sch} and the standard deviation σ_{sch}, we draw a random number p_{sch} from the normal distribution $\mathcal{N}(\mu_{\text{sch}}, \sigma_{\text{sch}})$ to schedule a splitting time, where $\ell_{\text{sch}}^{i-1} < p_{\text{sch}} \leq \ell_{\text{sch}}^i$ indicates selecting the scheduling time $P_{\text{sch}} = \ell_{\text{sch}}^i$. We set $P_{\text{sch}} = \ell_{\text{sch}}^n$ if $p_{\text{sch}} > \ell_{\text{sch}}^n$. At the scheduled splitting position, platoon members will detach one by one, starting from the

platoon tail, by increasing their gap from their immediate downstream vehicle.

Case Study and Numerical Experiments

In this section we conduct experiments in the simulation framework laid out in the previous section, where the trajectory of the subject vehicle is controlled by the proposed optimal control model. The simulation framework consists of a two-lane highway where the subject vehicle is assumed to be initially traveling on the right lane. The traveled path is composed of 20 road pieces, with two on-ramps in the first and eighteenth road pieces, and three off-ramps on the fourth and twelfth road pieces and the destination of the trip. The travel path is 10.8 km in length, where the first, fourth, twelfth, and eighteenth road pieces are 400, 300, 200, and 300 m in length, respectively, and the rest of the road pieces are 600 m in length. Recall that we consider a road piece to be homogeneous in macroscopic traffic conditions.

We quantify the implications of the optimal control model under different configurations of platooning (enabled or not) and lane changing (enabled or not) in different traffic environments. Specifically, we consider three traffic states of free-flow traffic, onset-of-congestion traffic, and congested traffic. In order to provide a realistic simulation environment under each traffic state, we set up a warm-up process during which we use the Greenberg fundamental diagram [67, 68] to create simulation instances under each traffic state. For details, refer to Appendix A.

For each traffic state, we run seven simulation scenarios, each scenario using a different controller for the subject vehicle, as displayed in Table 4. We implement two basic controllers: CF refers to the IDM car-following model and OC refers to a basic optimal control model. More sophisticated controllers are introduced by adding platooning and lane-changing capabilities to these two basic controllers: the suffix "_Mi" indicates the platooning capability, where the vehicle

is required to keep its platoon membership for at least i km if it merges into a platoon, the suffix "_L" refers to the lane-changing capability, and the suffix "_LMi" refers to a controller that has both platooning and lane-changing capabilities. Finally, for all seven controllers listed in Table 4, VoT is assumed to be zero, indicating that the generalized cost effectively turns into the fuel cost. we use the suffix "_Tj" at the end of the controllers to denote a non-zero VoT of j. For each traffic state, we run 25 random instances of each simulation scenario and report the trip cost, which is a linear combination of the fuel and time costs.

Efficiency Results for the Subject Vehicle

In this section we report the overall cost of the subject vehicle under the seven introduced controllers, the three traffic states, and two different VoTs. Figure 2 displays the results for the VoT $\eta_t = 0$ dollars per hour, effectively comparing the fuel efficiency benefits of the seven controllers. The values of the overall fuel consumption by the subject vehicle under all scenario pairs are compared using a two-tailed Student's t-tests at the 5% significance level to identify fuel savings that are statically significant.

The top plot in Figure 2 presents the results for the free-flow traffic state. These results suggest that without lane changing, the optimal control model both with and without the ability to form a platoon (i.e., OC, OC_M0, and OC_M6), can result in statistically significant reductions in fuel cost (at the 5% significance level), compared to the car-following model (CF). With lane changing, OC_L and OC_LM0 result in even higher fuel costs than CF. This is because the lane-changing process itself may add to the fuel cost—a cost that might be underestimated by the short-sighted OC. In general, if the subject vehicle is platoon enabled and forced to keep its platoon membership for at least 6 km (i.e., the OC_M6 and OC_LM6 scenarios), the fuel savings are more significant compared to OC alone. However, with lane changing, scenario OC_LM0, where the platoon can dissolve at any time after its formation, does not produce statistically significant fuel savings compared to OC_L. These results indicate that a stable, long-term platoon membership can have a positive effect on fuel efficiency.

The middle plot in Figure 2 demonstrates the results for the onset-of-congestion traffic state. Results indicate that similar to the free-flow case, without lane changing, optimal control offers statistically significant fuel savings compared to car-following for all control-based scenarios (with and without platooning). With lane changing, OC_L results in higher fuel cost compared with CF, and OC_LM0 has no significant difference with CF. However, a comparison of OC, OC_M0, and OC_M6 scenarios in the onset-of-congestion traffic state shows that OC_M0 results in the least fuel saving, OC holds the second place, while OC_M6 achieves the most fuel saving. These results are intuitive since the frequent splitting of the subject vehicle from platoons in the onset-of-congestion state leads to higher energy consumption in the

TABLE 4 List of controllers.

Controller	Description
CF	The intelligent driver car-following model [66]
OC	Optimal control model
OC_M0	OC with platoon merging, but no minimum required distance to travel in a platoon
OC_M6	OC with platoon merging, but a minimum required distance of 6 km to travel in a platoon
OC_L	OC with lane changing enabled
OC_LM0	OC_M0 with lane changing enabled
OC_LM6	OC_M6 with lane changing enabled

© SAE International

FIGURE 2   The top, middle, and bottom figures represent the free-flow, onset-of-congestion, and congested traffic states, respectively. The vertical axes in these figures show the overall costs in dollars for 10 km-long trips. Along the horizontal axes, the overall costs of the subject vehicle under different controllers are compared. The VoT is set to 0 dollars per hour in all simulations.
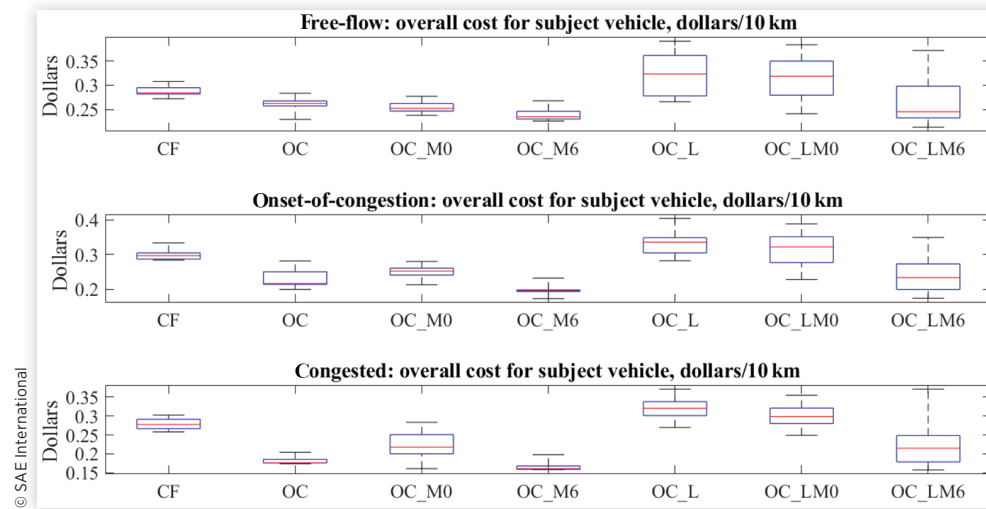
OC_M0 scenario, and the energy savings from a short-lived platoon cannot make up for this loss.

Finally, the bottom figure in Figure 2 displays the results for the congested traffic state. Results indicate that similar to the two previous traffic states, without lane changing, optimal control offers lower fuel costs compared to car-following. The OC_M0 controller does not offer statistically significant improvements over OC for the same reason stated above; however, OC_M6 can still offer statistically significant fuel savings over both OC and OC_M0.

In general, Figure 2 shows that regardless of traffic state, the OC can outperform the CF in terms of energy efficiency. Enabling platooning can increase these benefits even further if the model does not allow the platoon to dissolve right after its formation, and forces platoon members to travel together

for a period of time. Lane changing could reduce the fuel efficiency benefits of the optimal control controllers to the point of matching fuel efficiency levels of traditional CFs; however, when platoon-keeping is enforced, the undesirable fuel efficiency implications of lane changing can be negated to a great extent.

In Figure 3, we set the VoT to $20 per hour and conduct simulations similar to those in Figure 2. This figure shows that minimizing a generalized cost, which takes into account the driver's VoT in addition to fuel cost, turns lane changing into a more desirable feature of the OC.

Under a VoT of 20, in the congested traffic state, there is no significant difference among all seven controllers. In the free-flow traffic state, we observe no statistically significant difference among OC_L_T20, OC_LM0_T20, and

FIGURE 3   The generalized cost of a 10.8 km-long trip with a VoT of $20 per hour under various traffic states and controllers.
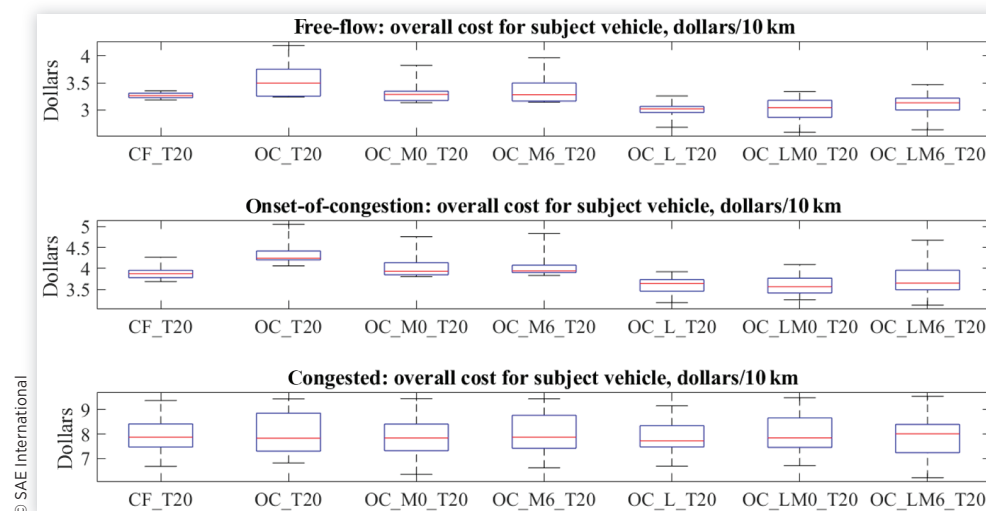
OC_LM6_T20, indicating that when lane changing is enabled, platooning does not induce a significant change in the generalized cost. This is mainly due to the lower fuel cost compared to the VoT. In the onset-of-congestion traffic state, the OC_LM6_T20 controller results in a slightly higher overall cost compared with OC_L_T20. It is due to the fact that when forcing a platoon to hold for 6 km, its members cannot change lanes, resulting in a larger time cost. In free-flow and onset-of-congestion traffic states, different from Figure 2, here the overall cost is reduced with lane changing. In both the free-flow and onset-of-congestion traffic states, OC_M0_T20 can result in significant overall cost savings compared with OC_T20, showcasing the importance of platooning in reducing the generalized cost, while OC_M6_T20 has no significant difference compared with OC_M0_T20.

By quantifying the effects of lane changing and platooning on the fuel and time costs, Figures 2 and 3 allow us to infer policies on the circumstances under which engaging in lane changing and/or platoon merging can reduce a vehicle's generalized cost of travel. In general, platooning reduces fuel cost and lane changing reduces the time cost of a trip. As such, the overall generalized cost becomes dependent on the relative values of the VoT and fuel cost—if the VoT is small compared to the fuel cost, the contribution of platooning to the generalized cost overweighs that of the time cost, indicating a cost-minimizing policy of merging into platoons, committing to them for long periods, and avoiding lane changes. On the other hand, if the VoT is large relative to the fuel cost, the time component of the generalized cost overweighs the fuel cost, resulting in the cost-minimizing policy of not blindly committing to a platoon for a long period, while taking advantage of lane changing to reduce travel time when possible.

Efficiency Results for the Surrounding Vehicles

In this section, we analyze the simulation results to investigate whether the different controllers used by the subject vehicle have a significant impact on the overall cost of its upstream traffic. We use the average cost of $N_{sur} = 30$ upstream vehicles of the subject vehicle in both lanes as an approximation of the cost of a surrounding vehicle. We assume that surrounding vehicles have the same VoT as the subject vehicle.

Figure 4 displays the average cost of $N_{sur} = 30$ upstream vehicles to the subject vehicle under the three traffic states and the seven controllers, with a VoT set to 0, thereby effectively measuring the impact of the controllers on fuel efficiency. This figure suggests that changing the subject vehicle controller from the CF to the OC may have different implications in fuel consumption of the upstream vehicles depending on the traffic state. More specifically, replacing CF with OC results in significant fuel savings for the surrounding vehicles in the free-flow traffic, does not introduce a significant change in the onset-of-congestion traffic state, and induces a significant rise in fuel consumption under the congested traffic state. This is due to the fact that when considering the OC and CF controllers, fuel saving originates from efficient cruising. As such, the higher the congestion level, the more abrupt changes in acceleration are required to maintain a safety gap, resulting in higher fuel costs. Vehicles upstream to the subject vehicle react to the subject vehicle's changes in velocity following a CF. As such, the oscillations in the velocity profile of the subject vehicle are directly transferred to them. This could result in a lack of fuel efficiency, or even rise in fuel consumption, for vehicles traveling upstream to the subject vehicle. As a result, the OC controller can provide statistically significant fuel savings under the free-flow state where smooth cruising is

FIGURE 4 Average fuel cost of the surrounding traffic under different traffic states and controllers. The surrounding traffic consists of a total of 30 vehicles upstream of the subject vehicle, with 15 vehicles in the right lane and 15 vehicles in the left lane.
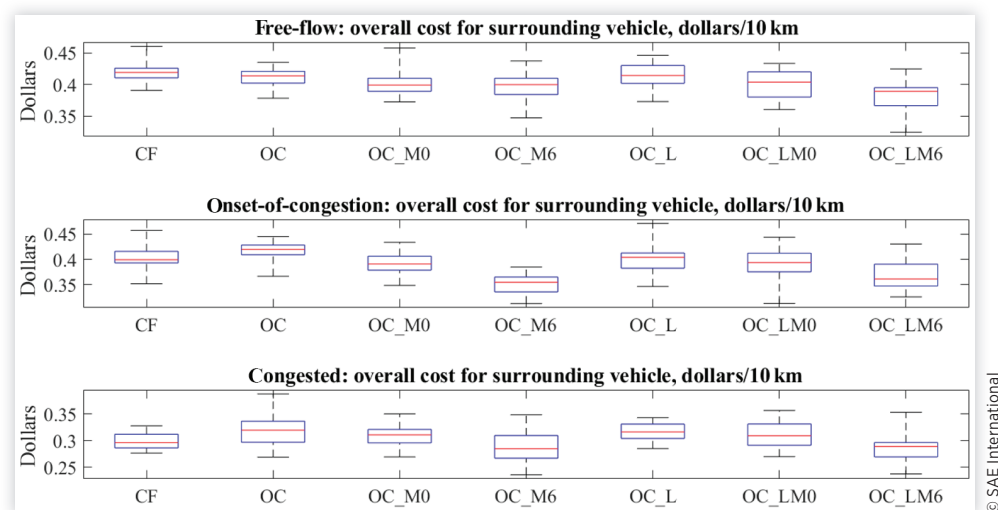
FIGURE 5   Average generalized cost of the surrounding traffic with a VoT of $20 per hour under different traffic states and controllers. The surrounding traffic consists of a total of 30 vehicles upstream of the subject vehicle, with 15 vehicles in the right lane and 15 vehicles in the left lane.
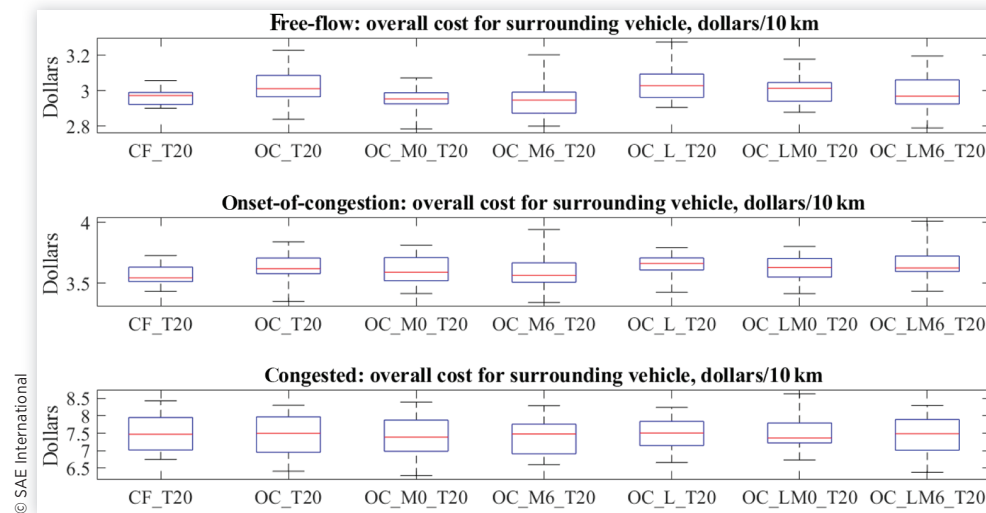
more likely to occur. These benefits disappear under the onset-of-congestion state, and are reversed under the congested state.

The controller OC_M6 outperforms CF, OC, and OC_M0 in all three traffic states, indicating that a CV can create fuel efficiency for its upstream traffic if it joins a platoon and commits to it. Similarly, when lane changing is enabled, OC_LM6 outperforms OC_L and OC_LM0, confirming the same conclusion. Among all controllers, OC_LM6 results in the most overall fuel savings for the surrounding vehicles. Finally, the subject vehicle's lane-changing decisions do not create a significant difference in the surrounding vehicles' fuel consumption.

In Figure 5, we set the VoT to $20 per hour for all vehicles. There is no statistically significant difference among controllers in the onset-of-congestion and congested traffic states. In the free-flow traffic state, OC_T20 and OC_L_T20 result in larger costs for the surrounding vehicles. This behavior results from the fact that under this high VoT, the time cost becomes the overwhelming portion of the total cost. As such, the subject vehicle's steady behavior under OC_M6_T20 or OC_LM6_T20 will not influence the surrounding vehicles, but a short-sighted controller will perturb the traffic and increase the time cost of surrounding vehicles. This influence is not statistically significant in the onset-of-congestion and congested traffic states because the time cost under OC is already significant.

Impact of Platooning

Figure 6 allows us to pinpoint the source of fuel efficiency induced by the proposed model. This figure shows the velocity curves of the subject vehicle and its immediate upstream vehicle in the onset-of-congestion traffic state in an example trip with a VoT of 0. The points at the bottom of the plots in this figure mark the platoon membership status of the subject vehicle under the OC_M6 and OC_M0 controllers at each time step. In Figure 6, only the first 500 s of the trip are presented, and the fuel costs for this 500 second-long section of the trip as well as the entire trip are shown in Table 5. This figure shows that, compared to CF, the OC provides smoother velocity curves, thereby resulting in fuel savings for both the subject vehicle and its immediate upstream vehicle. This figure also demonstrates that the OC_M6 controller provides the smoothest trajectories and, therefore, can provide the highest fuel-saving benefits.

Lane Changing and Its Impact

Figure 7 allows us to demonstrate how the subject vehicle makes lane-changing decisions. This figure shows the fuel consumption curves of the subject vehicle and those of its downstream vehicles (averaged over 30 vehicles) on both the right and left lanes for an example trip in the onset-of-congestion traffic state. The controller of the subject vehicle is set to OC_L. The solid green line indicates the lane in which the subject vehicle travels at each time step, where the value 1 indicates the left lane. At about 160 s, the subject vehicle changes from the left lane to the right lane. This lane change can be attributed to the lower fuel consumption of downstream traffic in the right lane at about 140 to 160 s. At about 245 s, the subject vehicle changes from the right lane to the left lane due to the lower fuel consumption of downstream traffic in the left lane at about 245 to 260 s. The subject vehicle again switches from the left lane to the right lane at about 290 s due to the lower fuel consumption in the right lane at about 275 to 290 s. As this figure shows, changing lanes in response to reductions in fuel consumption in the other lane may bring about short-term fuel savings, but the frequency of these lane changes may increase the total fuel cost, as was demonstrated and discussed previously.

FIGURE 6 The vertical axis shows velocity, with the unit of meters per second (m/s). The horizontal axis is time, with the unit of seconds (s). The top plot compares the speed curves of the subject vehicle under different controllers, and the bottom plot shows the corresponding speed curves of the immediate upstream vehicle to the subject vehicle.
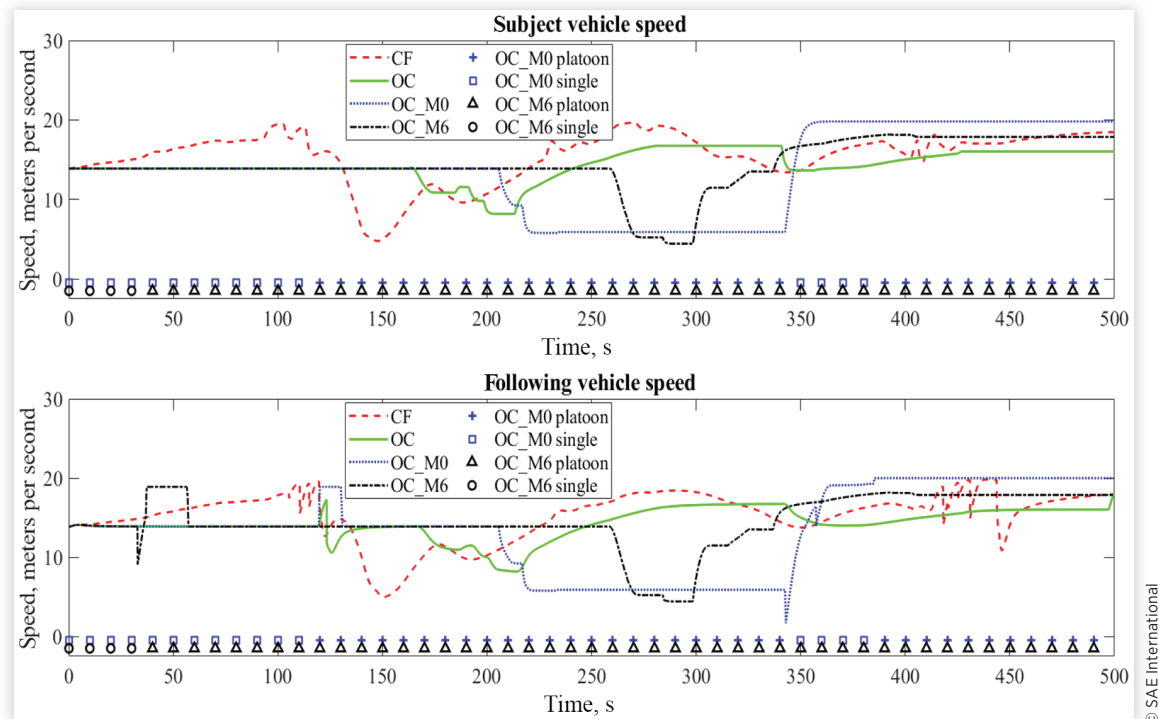

© SAE International

Figure 8 shows how the subject vehicle's lane-changing decisions can influence the fuel consumption of the upstream traffic in both lanes. This figure shows the fuel consumption curves of the subject vehicle and its upstream vehicles (in both lanes) in an example trip under the onset-of-congestion traffic state. The controller of the subject vehicle and the lane indicator are the same as in Figure 7. At about 380 s, the subject vehicle changes from the left lane to the right lane. Figure 8 shows that the subject vehicle switching to the right lane does not negatively affect the fuel consumption in that lane, explaining the general trends in Figure 4.

TABLE 5 Fuel cost for the subject vehicle and its immediate upstream vehicle in an example trip under the onset-of-congestion traffic state.

| Fuel cost, dollars per 10 km	First 500 s		The entire trip	
	Subject vehicle	Following vehicle	Subject vehicle	Following vehicle
CF	0.3096	0.3519	0.3045	0.3518
OC	0.2420	0.2592	0.2422	0.2753
OC_M0	0.2439	0.2614	0.2424	0.2556
OC_M6	0.2238	0.2431	0.2166	0.2295

© SAE International

Conclusion

In this article we proposed an optimal control model for trajectory planning of a CAV in a mixed traffic environment. The optimal controller was developed to plan the trajectory of the subject vehicle, including platoon formation and lane-changing decisions, while explicitly accounting for computation delay. The objective of the optimal control model was to minimize the generalized cost of a trip, which is a linear combination of its fuel and time costs. We developed a simulation framework to quantify the effectiveness of the optimal control model in providing first-hand cost savings for the subject vehicle as well as second-hand savings for the vehicles traveling upstream of the subject vehicle. Our experiments suggest that, generally speaking, the optimal controller outperforms the IDM car-following model in creating fuel efficiency. Results suggest that making platooning decisions based on local information does not necessarily lead to fuel savings; however, if a minimum platoon-keeping distance is enforced by the model, platooning can offer significant fuel-efficiency benefits, especially in the onset-of-congestion and congested traffic states. Our experiments also indicate that under the controller with enforced minimum platoon-keeping distance, the non-CVs upstream of the subject vehicle may also experience second-hand statistically significant fuel savings. When a generalized cost of travel including both the time and fuel cost is considered, lane

FIGURE 7 The vertical axis shows the fuel consumption, with the unit of dollars per 10 km. The horizontal axis is time, with the unit of seconds. The average fuel cost of vehicles downstream of the subject vehicle in both lanes (15 vehicles in the left lane and 15 vehicles in the right lane), and the fuel cost of the subject vehicle and its lane position are shown.
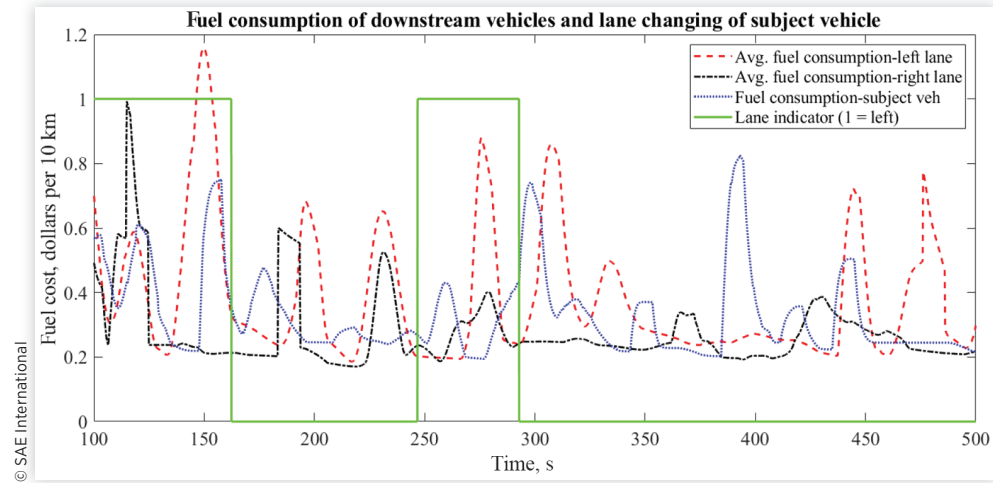
FIGURE 8 The vertical axis shows fuel consumption, with the unit of dollars per 10 km. The horizontal axis is time, with the unit of seconds. The average fuel cost of vehicles upstream of the subject vehicle in both lanes (15 vehicles in the left lane and 15 vehicles in the right lane), and the fuel cost of the subject vehicle and its lane position are shown.

329
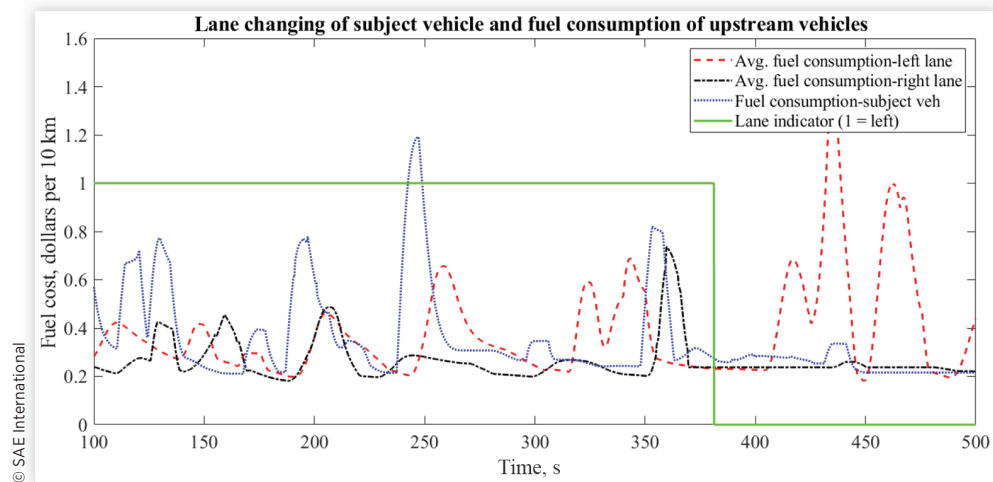
changing may introduce time savings significant enough to more than compensate the increased fuel consumption during the lane-change maneuver and, in fact, reduce the overall cost of a trip. As such, our experiments indicate the importance of the relative values of fuel cost and VoT in a driver's decision-making process—with a higher VoT, lane changing becomes more attractive, leading to the generalized cost preferring a shorter trip to a more fuel-efficient one. Similarly, with a smaller VoT one might benefit from merging into a platoon to reduce his/her fuel cost. This interesting relationship can open doors for introducing mechanisms between agents where those with lower VoTs might grant lane access to those with higher VoTs for monetary compensation, thereby increasing utilities of all parties.

Contact Information

Neda Masoud, Ph.D.
Assistant Professor
University of Michigan, Ann Arbor
Work Address: 2350 Hayward, 2124 GG Brown Ann Arbor, Michigan 48109-2125
nmasoud@umich.edu

References

1. Monteil, J., Billot, R., Sau, J., Armetta, F. et al., "Cooperative Highway Traffic: Multiagent Modeling and Robustness Assessment of Local Perturbations," *Transportation Research Record* 2391, no. 1 (2013): 1-10.

2. Ersal, T., Kolmanovsky, I., Masoud, N., Ozay, N. et al., "Connected and Automated Road Vehicles: State of the Art and Future Challenges," *Vehicle System Dynamics* 58, no. 5 (2020): 672-704.

3. S. O.-R. A. V. S. Committee et al., "Taxonomy and Definitions for Terms Related to On-Road Motor Vehicle Automated Driving Systems," *SAE Standard J* 3016 (2014): 1-16.

4. Zhang, Z., Tafreshian, A., and Masoud, N., "Modular Transit: Using Autonomy and Modularity to Improve Performance in Public Transportation," *Transportation Research Part E: Logistics and Transportation Review* 141 (2020): 102033.

5. Masoud, N. and Jayakrishnan, R., "Formulations for Optimal Shared Ownership and Use of Autonomous or Driverless Vehicles," in *Proceedings of the Transportation Research Board 95th Annual Meeting*, 1-17, Washington DC, USA, 2016.

6. van Wyk, F., Khojandi, A., and Masoud, N., "Optimal Switching Policy between Driving Entities in Semi-Autonomous Vehicles," *Transportation Research Part C: Emerging Technologies* 114 (2020): 517-531.

7. Masoud, N. and Jayakrishnan, R., "Autonomous or Driver-Less Vehicles: Implementation Strategies and Operational Concerns," *Transportation Research Part E: Logistics and Transportation Review* 108 (2017): 179-194.

8. van Wyk F., Khojandi A., and Masoud N., "A Path Towards Understanding Factors Affecting Crash Severity in Autonomous Vehicles Using Current Naturalistic Driving Data," in *Proceedings of SAI Intelligent Systems Conference*, 106-120, Springer, Cham, London, UK, 2019.

9. Gasparetto, A., Boscariol, P., Lanzutti, A., and Vidoni, R., "Path Planning and Trajectory Planning Algorithms: A General Overview," *Motion and operation planning of robotic systems*, 3-27, Mechanisms and Machine Science, vol 29. Springer, Cham. Switzerland, 2015.

10. Zhang, S., Deng, W., Zhao, Q., Sun, H., and Litkouhi, B., "Dynamic Trajectory Planning for Vehicle Autonomous Driving," in *2013 IEEE International Conference on Systems, Man, and Cybernetics*, Manchester, UK, 4161-4166, Oct 2013.

11. Zeng, X. and Wang, J., "Globally Energy-Optimal Speed Planning for Road Vehicles on a Given Route," *Transportation Research Part C Emerging Technologies* 93 (2018): 148-160.

12. Han, Y.L., "On Generating Driving Trajectories in Urban Traffic to Achieve Higher Fuel Efficiency," M.S. thesis, University of Illinois at Urbana-Champaign, Urbana-Champaign, USA, 2014.

13. Yu, K., Tan, X., Yang, H., Liu, W. et al., "Model Predictive Control of Hybrid Electric Vehicles for Improved Fuel Economy: Mpc of Hevs for Improved Fuel Economy," *Asian Journal of Control* 18, no. 6 (2016): 2122-2135.

14. Lee, S.H., "Intelligent Techniques for Improved Engine Fuel Economy," PhD thesis, University of Brighton, Brighton, UK, (2011).

15. Ozatay, E., Ozguner, U., and Filev, D., "Velocity Profile Optimization of on Road Vehicles: Pontryagin's Maximum Principle Based Approach," *Control Engineering Practice* 61 (2017): 244-254.

16. Lipp, T. and Boyd, S., "Minimum-Time Speed Optimisation over a Fixed Path," *International Journal of Control* 87, no. 6 (2014): 1297-1311.

17. Ebbesen, S., Salazar, M., Elbert, P., Bussi, C. et al., "Time-Optimal Control Strategies for a Hybrid Electric Race Car," *IEEE Transactions on Control Systems Technology* 26, no. 1 (2017): 233-247.

18. Abdolmaleki, M., Masoud, N., and Yin, Y., "Vehicle-to-Vehicle Wireless Power Transfer: Paving the Way toward an Electrified Transportation System," *Transportation Research Part C: Emerging Technologies* 103 (2019): 261-280.

19. Werling, M., Ziegler, J., Kammel, S., and Thrun, S., "Optimal Trajectory Generation for Dynamic Street Scenarios in a Frenet Frame," in *2010 IEEE International Conference on Robotics and Automation*, Anchorage, Alaska, USA, 987-993, IEEE, 2010.

20. Karaman, S. and Frazzoli, E., "Optimal Kinodynamic Motion Planning Using Incremental Sampling-Based Methods," in *49th IEEE Conference on Decision and Control (CDC)*, Atlanta, Georgia, USA, 7681-7687, IEEE, 2010.

21. Meng, Y., Wu, Y., Gu, Q., and Liu, L., "A Decoupled Trajectory Planning Framework Based on the Integration of Lattice Searching and Convex Optimization," *IEEE Access* 7 (2019): 130530-130551.

22. Luo, Y., Xiang, Y., Cao, K., and Li, K., "A Dynamic Automated Lane Change Maneuver Based on Vehicle-to-Vehicle Communication," *Transportation Research Part C* 62 (2016): 87-102.

23. Stahl, T., Wischnewski, A., Betz, J., and Lienkamp, M., "Multilayer Graph-Based Trajectory Planning for Race Vehicles in Dynamic Scenarios," in *2019 IEEE Intelligent Transportation Systems Conference (ITSC)*, Auckland, NZ, 3149-3154, IEEE, 2019.

24. Gu, T., Dolan, J.M., and Lee, J.W., *On-Road Trajectory Planning for General Autonomous Driving with Enhanced Tunability* (Springer International Publishing, 2016)

25. Hu, X., Chen, L., Tang, B., Cao, D. et al., "Dynamic Path Planning for Autonomous Driving on Various Roads with Avoidance of Static and Moving Obstacles," *Mechanical Systems and Signal Processing* 100 (2018): 482-500.

26. Huang, Z., Chu, D., Wu, C., and He, Y., "Path Planning and Cooperative Control for Automated Vehicle Platoon Using Hybrid Automata," *IEEE Transactions on Intelligent Transportation Systems* 20 (March 2019): 959-974.

27. Plessen, M.G., "Trajectory Planning of Automated Vehicles in Tube-Like Road Segments," in *2017 IEEE 20th International Conference on Intelligent Transportation Systems (ITSC)*, 1-6, Oct 2017.

28. Ntousakis, I.A., Nikolos, I.K., and Papageorgiou, M., "Optimal Vehicle Trajectory Planning in the Context of Cooperative Merging on Highways," *Transportation Research Part C: Emerging Technologies* 71 (2016): 464-488.

29. Gritschneder F., Graichen K., and Dietmayer K., "Fast Trajectory Planning for Automated Vehicles Using Gradient-Based Nonlinear Model Predictive Control," 2018, IEEE/RSJ International Conference on Intelligent Robots and Systems (IROS), 7369-7374. IEEE, Madrid, Spain, 2018.

30. McNaughton, M., Urmson, C., Dolan, J.M., and Lee, J.-W., "Motion Planning for Autonomous Driving with a Conformal Spatiotemporal Lattice," in *2011 IEEE International Conference on Robotics and Automation*, Shanghai, China, 4889-4895, IEEE, 2011.

31. Herrmann, T., Wischnewski, A., Hermansdorfer, L., Betz, J. et al., "Real-Time Adaptive Velocity Optimization for Autonomous Electric Cars at the Limits of Handling," *IEEE Transactions on Intelligent Vehicles* (2020), https://doi.org/10.1109/TIV.2020.3047858.

32. Zhang, L. and Orosz, G., "Designing Network Motifs in Connected Vehicle Systems: Delay Effects and Stability," in *ASME Dynamic Systems and Control Conference*, Palo Alto, CA, USA, V003T42A006-V003T42A006, 2013.

33. Orosz, G., "Connected Cruise Control: Modelling, Delay Effects, and Nonlinear Behaviour," *Vehicle System Dynamics* 54, no. 8 (2016): 1147-1176.

34. Zhang, L., Sun, J., and Orosz, G., "Hierarchical Design of Connected Cruise Control in the Presence of Information Delays and Uncertain Vehicle Dynamics," *IEEE Transactions on Control Systems Technology* 99 (2018): 1-12.

35. Ge, J.I. and Orosz, G., "Optimal Control of Connected Vehicle Systems with Communication Delay and Driver Reaction Time," *IEEE Transactions on Intelligent Transportation Systems* 99 (2017): 1-15.

36. Dey, K.C., Yan, L., Wang, X., Wang, Y. et al., "A Review of Communication, Driver Characteristics, and Controls Aspects of Cooperative Adaptive Cruise Control (Cacc)," *IEEE Transactions on Intelligent Transportation Systems* 17 (Feb 2016): 491-509.

37. Milanés, V. and Shladover, S.E., "Modeling Cooperative and Autonomous Adaptive Cruise Control Dynamic Responses Using Experimental Data," *Transportation Research Part C: Emerging Technologies* 48 (2014): 285-300.

38. Wischhof, L., Ebner, A., and Rohling, H., "Information Dissemination in Self-Organizing Intervehicle Networks," *IEEE Transactions on intelligent transportation systems* 6, no. 1 (2005): 90-101.

39. Zheng, Y., Li, S.E., Wang, J., Wang, L.Y., and Li, K., "Influence of Information Flow Topology on Closed-Loop Stability of Vehicle Platoon with Rigid Formation," in *17th International IEEE Conference on Intelligent Transportation Systems (ITSC)*, Qingdao, China, 2094-2100, IEEE, 2014.

40. Fan, B. and Krishnan, H., "Reliability Analysis of Dsrc Wireless Communication for Vehicle Safety Applications," 2006, IEEE intelligent transportation systems conference, 355-362. IEEE, Toronto, Ontario, Canada, 2006.

41. Uhlemann, E., "Connected-Vehicles Applications Are Emerging [Connected Vehicles]," *IEEE Vehicular Technology Magazine* 11, no. 1 (2016): 25-96.

42. Sánchez, M.G. and Táboas, M.P., "Millimeter Wave Radio Channel Characterization for 5g Vehicle-to-Vehicle Communications," *Measurement* 95 (2017): 223-229.

43. Paden, B., Čáp, M., Yong, S.Z., Yershov, D. et al., "A Survey of Motion Planning and Control Techniques for Self-Driving Urban Vehicles," *IEEE Transactions on intelligent vehicles* 1, no. 1 (2016): 33-55.

44. Claussmann L., Revilloud M., Gruyer D., and Glaser S., "A Review of Motion Planning for Highway Autonomous Driving," *IEEE Transactions on Intelligent Transportation Systems*, 2019.

45. Talebpour, A., Mahmassani, H.S., and Hamdar, S.H., "Modeling Lane-Changing Behavior in a Connected Environment: A Game Theory Approach," *Transportation Research Procedia*, vol. 7, pp. 420-440, 2015. in *21st International Symposium on Transportation and Traffic Theory Kobe*, Japan, 5-7 August 2015.

46. Desiraju, D., Chantem, T., and Heaslip, K., "Minimizing the Disruption of Traffic Flow of Automated Vehicles during Lane Changes," *IEEE Transactions on Intelligent Transportation Systems* 16, no. 3 (2014): 1249-1258.

47. Rahman, M., Chowdhury, M., Xie, Y., and He, Y., "Review of Microscopic Lane-Changing Models and Future Research Opportunities," *IEEE Transactions on Intelligent Transportation Systems* 14, no. 4 (2013): 1942-1956.

48. Zheng, Z., "Recent Developments and Research Needs in Modeling Lane Changing," *Transportation Research Part B* 60, no. 1 (2014): 16-32.

49. Wang M., Hoogendoorn S.P., Daamen W., van Arem B., and Happee R., "Game Theoretic Approach for Predictive Lane-Changing and Car-Following Control," *Transportation Research Part C: Emerging Technologies*, vol. 58, pp. 73-92, 2015.

50. Nilsson, J., Silvlin, J., Brannstrom, M., Coelingh, E. et al., "If, when, and how to Perform Lane Change Maneuvers on Highways," *IEEE Intelligent Transportation Systems Magazine* 8, no. 4 (2016): 68-78.

51. Zabat, M., "The Aerodynamic Performance of Platoon: Final Report," *California Path Research Report*, 1995.

52. Alam, A., Besselink, B., Turri, V., Martensson, J. et al., "Heavy-Duty Vehicle Platooning for Sustainable Freight Transportation: A Cooperative Method to Enhance Safety and Efficiency," *IEEE Control Systems* 35, no. 6 (2015): 34-56.

53. Farnsworth, S.P., "El Paso Comprehensive Modal Emissions Model (CMEM) Case Study," *Automobiles* (2001).

54. Shladover, S.E., Nowakowski, C., Lu, X.Y., and Ferlis, R., "Cooperative Adaptive Cruise Control (CACC) Definitions and Operating Concepts," in *Proceedings of the Transportation Research Board 94th Annual Meeting*, Washington DC, USA, 2015.

55. Lioris, J., Pedarsani, R., Tascikaraoglu, F.Y., and Varaiya, P., "Platoons of Connected Vehicles Can Double Throughput in Urban Roads," *Transportation Research Part C: Emerging Technologies* 77 (2017): 292-305.

56. Contet, J.M., Gechter, F., Gruer, P., and Koukam, A., "Bending Virtual Spring-Damper: A Solution to Improve Local Platoon Control," in *International Conference on Computational Science*, 601-610, 2009.

57. Guo, G. and Yue, W., "Hierarchical Platoon Control with Heterogeneous Information Feedback," *Control Theory & Applications Iet* 5, no. 15 (2011): 1766-1781.

58. El-Zaher, M., Dafflon, B., Gechter, F., and Contet, J.M., "Vehicle Platoon Control with Multi-Configuration Ability," *Procedia Computer Science* 9, no. 11 (2012): 1503-1512.

59. Maiti, S., Winter, S., and Kulik, L., "A Conceptualization of Vehicle Platoons and Platoon Operations," *Transportation Research Part C Emerging Technologies* 80 (2017): 1-19.

60. Katrakazas, C., Quddus, M., Chen, W.-H., and Deka, L., "Real-Time Motion Planning Methods for Autonomous on-Road Driving: State-of-the-Art and Future Research Directions," *Transportation Research Part C: Emerging Technologies* 60 (2015): 416-442.

61. González, D., Pérez, J., Milanés, V., and Nashashibi, F., "A Review of Motion Planning Techniques for Automated Vehicles," *IEEE Transactions on Intelligent Transportation Systems* 17, no. 4 (2015): 1135-1145.

62. Makantasis, K. and Papageorgiou, M., "Motorway Path Planning for Automated Road Vehicles Based on Optimal Control Methods," *Transportation Research Record* 2672, no. 19 (2018): 112-123.

63. Gillespie, T.D., "Fundamentals of Vehicle Dynamics," tech. rep., SAE Technical Paper 1992.

64. Basak, K., Hetu, S.N., Azevedo, C.L., Loganathan, H., Toledo, T., Ben-Akiva, M., et al., "Modeling Reaction Time within a Traffic Simulation Model," in *16th International IEEE Conference on Intelligent Transportation Systems (ITSC 2013)*, The Hague, The Netherlands, 302-309, IEEE, 2013.

65. Molnár, T.G., Qin, W.B., Insperger, T., and Orosz, G., "Application of Predictor Feedback to Compensate Time Delays in Connected Cruise Control," *IEEE Transactions on Intelligent Transportation Systems* 19, no. 2 (2017): 545-559.

66. Jin, I.G. and Orosz, G., "Optimal Control of Connected Vehicle Systems with Communication Delay and Driver Reaction Time," *IEEE Transactions on Intelligent Transportation Systems* 18, no. 8 (2016): 2056-2070.

67. Greenshields, B., Channing, W., Miller, H., et al., "A Study of Traffic Capacity," in *Highway Research Board Proceedings*, vol. 1935, National Research Council (USA), Highway Research Board, Washington DC, USA, 1935.

68. Pipes, L.A., "Car Following Models and the Fundamental Diagram of Road Traffic," *Transportation Research/UK*, 1966.

69. Qu, X., Zhang, J., and Wang, S., "On the Stochastic Fundamental Diagram for Freeway Traffic: Model Development, Analytical Properties, Validation, and Extensive Applications," *Transportation Research Part B: Methodological* 104 (2017): 256-271.

Appendix A. Simulation Warm-Up

According to [69], many different models have been proposed to capture the relationship among the three fundamental parameters of traffic flow—traffic flow, speed, and traffic density. Here we adopt Greenberg's model, which presents one of the earliest and most well-known speed-density models [67, 68]. Let v_m and k_m be the corresponding velocity and density when the flow reaches its maximum value, which is $\frac{1}{t_p}$. We set $k_1 = 0.3\,k_m$, $k_2 = 0.8\,k_m$, and $k_3 = 2\,k_m$ as the maximum density under the free-flow, onset-of-congestion, and congested traffic states, respectively. We then use Greenberg's speed-density relationship in Equation A.1 to compute the corresponding velocity of each of the three density cut-off points,

$$v = v_m \ln\left(\frac{k_j}{k}\right) \qquad\qquad \text{Eq. (A.1)}$$

where v denotes the space-mean speed, k denotes the traffic density, v_m indicates the velocity when the flow reaches its maximum value, and k_j indicates the jam density. The value of k_j is determined by the parameters in the IDM,

$$k_j = \frac{1}{l_{car} + h_{st}}$$
                                                          Eq. (A.2)

where l_{car} is the average vehicle length, and h_{st} is the minimum headway at which vehicles are at a complete stop. After generating vehicle positions using the ideal time gap, we perturb these positions using Gaussian noise to incorporate random deviations from an idealized model. During the warm-up process, all surrounding vehicles run for 2 min following the IDM.